Photoproduction of dileptons, photons, and light vector mesons in ultrarelativistic heavy ion collisions

Gong-Ming Yu and Yun-De Li
Department of Physics, Yunnan University, Kunming 650091, China
(Received 30 August 2014; revised manuscript received 10 March 2015; published 28 April 2015)

We calculate the production cross section for dileptons, photons, and light vector mesons (ρ, ω, and ϕ) produced by the photoproduction processes in relativistic heavy ion collisions. The jet-quenching effects for fragmentation processes with $p_T > 2$ GeV and the jet-medium interaction with $p_T > 4$ GeV for the fast jets passing through the quark-gluon plasma in Pb-Pb collisions are also considered. The numerical results of photoproduction processes can improve the contribution of dileptons, photons, and light vector meson production in p-p and Pb-Pb collisions at Large Hadron Collider energies.

DOI: 10.1103/PhysRevC.91.044908 PACS number(s): 12.39.St, 25.75.−q, 21.65.Qr, 12.38.Mh

I. INTRODUCTION

Hadronic processes for large transverse momentum dileptons, photons, and light vector meson production is a vital goal in ultrarelativistic heavy ion collisions at the Large Hadron Collider (LHC). Since dileptons and photons do not participate in the strong interaction directly thus they will have no final-state interactions in a strongly interacting system with an electromagnetic mean-free path that is much larger than the typical size of this system [quark-gluon plasma (QGP)]. Hence dileptons and photons have long been proposed as ideal probes in the study of hot-dense nuclear matter. Moreover, the light vector meson production in p-p collisions is important as a baseline for heavy ion studies.

Recently, the measurement of dileptons, photons, and light vector mesons (ρ, ω, and ϕ) at LHC energies was performed by the ALICE Collaboration [1–5] and CMS Collaboration [6,7] for p-p collisions with $\sqrt{s_{NN}} = 7.0$ TeV and Pb-Pb collisions with $\sqrt{s_{NN}} = 2.76$ TeV. Furthermore, a big enhancement is shown in ALICE Collaboration direct photon data that cannot be interpreted by perturbative quantum chromodynamics (pQCD) next-to-leading-order results for $p_T < 4$ GeV with $\sqrt{s} = 2.76$ TeV [2]. In recent years, various processes of dileptons, photons, and light vector meson production in relativistic heavy ion collisions have been proposed: primary hard photons from initial parton collisions [8–14], photon-photon collisions in ultraperipheral collisions [15,16], thermal parton interaction in the QGP [17–23], hadronic gas [24–26], hadronic decays after freeze-out [27], jet-medium interaction in the thermal medium [28–36], the color glass condensate [37–39], and the preequilibrium Glasma stage [40,41], the purely diffractive mechanism that a real or virtual photon fluctuates into a vector meson through the exchange of the pomeron [42–44], the double diffractive process (Balitzkij-Fadin-Kuraev-Lipatov effects) [45,46], the recombination of thermal partons [47], and the dynamical quark coalescence based on the multiphase transport model [48].

In the present paper, we extend the photoproduction mechanism which plays a fundamental role in the ep deep inelastic scattering at the Hadron Electron Ring Accelerator [49–51] to the dileptons, photons, and light vector meson production in p-p collisions and Pb-Pb collisions at LHC energies. At high energies, the nucleus or the charged partons can emit high-energy photons (and hadronlike photons) in relativistic nucleus-nucleus collisions. The photoproduction processes may be direct and resolved which are sensitive to the gluon distribution in the nucleus. In the direct photoproduction processes, the high-energy photon emitted from the nucleus or the charged parton of the incident nucleus interacts with the parton of another incident nucleus by the interaction of quark-photon Compton scattering and gluon-photon fusion. In the resolved photoproduction processes, the uncertainty principle allows the high-energy hadronlike photon for a short time to fluctuate into a quark-antiquark pair which then interacts with the partons of another incident nucleus by quark-antiquark annihilation, quark-gluon Compton scattering, and gluon-gluon fusion. For the fragmentation processes and jet-medium interaction processes, the high-energy photon from the nucleus or the charged partons will interact with the partons of another incident nucleus by the interaction of $\gamma + q(g) \rightarrow$ jets for direct photoproduction processes, and the partons of the high-energy hadronlike photon can interact with the partons of another incident nucleus by $q + \bar{q} \rightarrow$ jets and $q + g \rightarrow$ jets for the resolved photoproduction processes. Subsequently the quark (or gluon) jets can pass through the quark-gluon plasma and lose their energy before fragmenting into dileptons, photons, light vector mesons, or interacting with the thermal partons of the hot-dense medium (jet-quenching effects).

The paper is organized as follows. In Sec. II we present the production of large-p_T dileptons and photons in p-p collisions and Pb-Pb collisions. The inelastic, semielastic, and elastic photoproduction processes are presented. The production rate of fragmentation and jet-dilepton (photon) conversion which includes the jet-quenching effects is also discussed. In Sec. III we investigate the production of light vector mesons from the photoproduction processes. The numerical results for p-p and Pb-Pb collisions at LHC energies are plotted in Sec. IV. Finally, a conclusion is given in Sec. V.

II. PHOTOPRODUCTION PROCESSES FOR LARGE-p_T DILEPTONS AND PHOTONS

Since photons and dileptons do not participate in the strong interaction directly, the photon or dilepton production can probe the strong interacting matter (QGP). We consider in our

 ©2015 American Physical Society

calculation that the dileptons and photons can be produced by the elastic, semielastic, and inelastic photoproduction processes in relativistic heavy ion collisions.

A. Large-p_T dilepton production

The dileptons can be produced by the initial parton collisions(the annihilation and Compton scattering of partons). The cross section for dileptons produced by the initial parton hard scattering processes (dir-fra.) in hadronic collisions can be written as [9]

$$\frac{d\sigma_{AB\to\ell^+\ell^-X}}{dM^2dp_T^2dy} = \int dx_a f_A(x_a,Q^2) f_B(x_b,Q^2)\frac{x_a x_b}{x_a - x_1} \times \frac{\alpha}{3\pi M^2}\sqrt{1-\frac{4m_\ell^2}{M^2}}\left(1+\frac{2m_\ell^2}{M^2}\right)\frac{d\hat{\sigma}_{ab\to\gamma^* d}}{d\hat{t}}, \tag{1}$$

where $x_b = (x_a x_2 - \tau)/(x_a - x_1)$ is the parton's momentum fraction. The variables are $x_1 = \frac{1}{2}(x_T^2 + 4\tau)^{1/2}\exp(y)$, $x_2 = \frac{1}{2}(x_T^2+4\tau)^{1/2}\exp(-y)$, $x_T = 2p_T/\sqrt{s}$, and $\tau = M^2/s$, and y is the rapidity. $d\hat{\sigma}/d\hat{t}(ab\to\gamma^* d)$ denotes the differential cross section of subprocesses,

$$\frac{d\hat{\sigma}}{d\hat{t}}(q\bar{q}\to\gamma^* g) = \frac{8}{9}\frac{\pi\alpha\alpha_s e_f^2}{\hat{s}^2}\left(\frac{\hat{t}}{\hat{u}}+\frac{\hat{u}}{\hat{t}}+\frac{2M^2\hat{s}}{\hat{t}\hat{u}}\right), \tag{2}$$

$$\frac{d\hat{\sigma}}{d\hat{t}}(q\bar{q}\to\gamma^*\gamma) = \frac{2}{3}\frac{\pi\alpha^2 e_f^4}{\hat{s}^2}\left(\frac{\hat{t}}{\hat{u}}+\frac{\hat{u}}{\hat{t}}+\frac{2M^2\hat{s}}{\hat{t}\hat{u}}\right), \tag{3}$$

$$\frac{d\hat{\sigma}}{d\hat{t}}(qg\to\gamma^* q) = \frac{1}{3}\frac{\pi\alpha\alpha_s e_f^2}{\hat{s}^2}\left(-\frac{\hat{u}}{\hat{s}}-\frac{\hat{s}}{\hat{u}}-\frac{2M^2\hat{t}}{\hat{s}\hat{u}}\right), \tag{4}$$

where $\hat{s} = (p_a+p_b)^2$, $\hat{t} = (p_c - p_a)^2$, and $\hat{u} = (p_c - p_b)^2$ are the Mandelstam variables for the subprocesses and M is the invariant mass of dileptons.

The parton distribution function $f_A(x_i,Q^2)$ of the nucleon is given by [52,53]

$$f_A(x_i,Q^2) = R_A(x_i,Q^2)\left[\frac{Z}{A}p(x_i,Q^2)+\frac{N}{A}n(x_i,Q^2)\right], \tag{5}$$

where $R_A(x_i,Q^2)$ is the nuclear modification factor [54], Z is the proton number, N is the neutron number, and A is the nucleon number; $p(x_i,Q^2)$ and $n(x_i,Q^2)$ are the parton distribution functions of protons and neutrons, respectively.

The large-p_T dileptons produced by semielastic photoproduction processes can be divided into the semielastic direct photoproduction processes (semi.dir-fra.) and semielastic resolved photoproduction processes (semi.res-fra.).

In the semielastic direct photoproduction processes (semi.dir.), incident nucleus A can emit a photon, then the high-energy photon interacts with parton b of another incident nucleus B by the interactions of quark-photon Compton scattering. The cross section of a dilepton produced by the semi.dir. can be written as

$$\frac{d\sigma^{\text{semi.dir.}}_{AB\to\ell^+\ell^-X}}{dM^2dp_T^2dy} = 2\int dx_a f_{\gamma/N}(x_a) f_B(x_b,Q^2)\frac{x_a x_b}{x_a - x_1} \times \frac{\alpha}{3\pi M^2}\sqrt{1-\frac{4m_\ell^2}{M^2}}\left(1+\frac{2m_\ell^2}{M^2}\right)\frac{d\hat{\sigma}_{\gamma b\to\gamma^* d}}{d\hat{t}}, \tag{6}$$

where $d\hat{\sigma}/d\hat{t}(\gamma b\to\gamma^* d)$ denotes the differential cross section of subprocesses,

$$\frac{d\hat{\sigma}}{d\hat{t}}(q\gamma\to\gamma^* q) = \frac{2\pi\alpha^2 e_f^4}{\hat{s}^2}\left(-\frac{\hat{u}}{\hat{s}}-\frac{\hat{s}}{\hat{u}}+\frac{2M^2\hat{t}}{\hat{s}\hat{u}}\right), \tag{7}$$

where $\hat{s} = (p_a+p_b)^2$, $\hat{t} = (p_c-p_a)^2$, and $\hat{u} = (p_c-p_b)^2$ are the Mandelstam variables for the subprocesses and M is the invariant mass of dileptons.

In the semielastic resolved photoproduction processes (semi.res.), parton a' from the resolved photon emitted by incident nucleus A can interact with parton b of another incident nucleus B via the interactions of quark-antiquark annihilation and quark-gluon Compton scattering. The large-p_T dileptons produced by the semi.res. in the hadronic collisions satisfy the following invariant cross section:

$$\frac{d\sigma^{\text{semi.res.}}_{AB\to\ell^+\ell^-X}}{dM^2dp_T^2dy} = 2\int dx_a dx_b f_{\gamma/A}(x_a) f_B(x_b,Q^2) \times f_\gamma(z_a,Q^2)\frac{x_a x_b z_a}{x_a x_b - x_a x_2}\frac{\alpha}{3\pi M^2}\sqrt{1-\frac{4m_\ell^2}{M^2}} \times\left(1+\frac{2m_\ell^2}{M^2}\right)\frac{d\hat{\sigma}_{a'b\to\gamma^* d}}{d\hat{t}}, \tag{8}$$

where $f_\gamma(z_a,Q^2)$ is the parton distribution function of the resolved photon [55].

For a charged ion moving with a relativistic factor $\gamma \gg 1$, only the electromagnetic field is present, and it attains large values since the nuclear charge then acts as a whole. At $Q^2 \sim 1/b^2 \sim 1/R^2$ the form factor is still not zero, the photon spectrum of a pointlike nucleus with a cutoff at $Q^2 \approx 1/R^2$ was used which is equivalent to neglecting the nuclear size for high-energy heavy ion collisions, where b is the impact parameters and R is the radius of the nucleus. The equivalent photon spectrum function for the nucleus can be obtained from a semiclassical description of high-energy electromagnetic collisions. A relativistic nucleus with Z times the electric charge moving with a relativistic factor $\gamma \gg 1$ with respect to some observer develops an equally strong magnetic-field component; hence, it resembles a beam of real photons where the photon spectrum function of low photon energies can be written as [56,57]

$$f_{\gamma/N}(\omega) = \frac{2Z^2\alpha}{\pi\omega}\ln\left(\frac{\gamma}{\omega R}\right), \tag{9}$$

where ω is the photon's momentum and $R = b_{\min}$ is the radius of the nucleus ($b_{\min}$ is the cutoff of impact). In the logarithmic approximation, the results obtained by a purely classical treatment or by including the form factor are related to each other through a rescaling of the relativistic factor (γ).

For p-p collisions, the equivalent photon spectrum function of a proton can be obtained from the Weizsäcker-Williams approximation [58–60],

$$f_{\gamma/p}(x) = \frac{\alpha}{2\pi x}[1+(1-x)^2] \times \left[\ln A - \frac{11}{6} + \frac{3}{A} - \frac{3}{2A^2} + \frac{1}{3A^3}\right], \quad (10)$$

where x is the photon's momentum fraction, m_p is the mass of the proton, $A = 1 + 0.71\ \mathrm{GeV}^2/Q^2_{\min}$ with

$$Q^2_{\min} = -2m_p^2 + \frac{1}{2s}\big[\big(s+m_p^2\big)\big(s-xs+m_p^2\big) - \big(s-m_p^2\big)\sqrt{\big(s-xs-m_p^2\big)^2 - 4m_p^2 xs}\big], \quad (11)$$

at high energies $Q^2_{\min}$ is given to a very good approximation by $m_p^2x^2/(1-x)$. Propagated uncertainties to the final cross sections are on the order of 10% for p-p collisions and 20% for Pb-Pb collisions since covering different form-factor parametrizations and the convolution of the nuclear photon fluxes [15].

The inelastic photoproduction physics for producing dileptons is very important in the research of relativistic heavy ion collisions. The inelastic photoproduction processes can be divided into three categories: inelastic direct photoproduction processes (inel.dir-fra.), inelastic resolved photoproduction processes (inel.res-fra.), and inelastic two-photon processes (inel.dou-fra.).

In the inelastic direct photoproduction processes, the photon from parton a of nucleus A interacts with parton b from nucleus B via the photon-quark interaction. The invariant cross section for large-p_T dilepton production by the inel.dir-fra. can be written as

$$\frac{d\sigma^{\text{inel.dir.}}_{AB\to\ell^+\ell^-X}}{dM^2dp_T^2dy} = 2\int dx_a dx_b f_A(x_a,Q^2) f_B(x_b,Q^2) \times f_{\gamma/q}(z_a)\frac{x_a x_b z_a}{x_a x_b - x_a x_2}\frac{\alpha}{3\pi M^2}\left(1+\frac{2m_\ell^2}{M^2}\right) \times\sqrt{1-\frac{4m_\ell^2}{M^2}}\frac{d\hat\sigma_{\gamma b\to\gamma^* d}}{d\hat t}, \quad (12)$$

where z_a is the photon's momentum fraction.

The equivalent photon spectrum function of a parton is given by [61–63]

$$f_{\gamma/q}(x) = \frac{\alpha}{\pi}e_f^2\left\{\frac{1+(1-x)^2}{x}\left[\ln\left(\frac{E}{m}\right) - \frac{1}{2}\right] + \frac{x}{2}\left[\ln\left(\frac{2}{x}-2\right)+1\right] + \frac{(2-x)^2}{2x}\ln\left(\frac{2-2x}{2-x}\right)\right\}, \quad (13)$$

where x is the photon's momentum fraction, e_f, E, and m are the charge, energy, and mass of the parton, respectively.

In the inelastic resolved photoproduction processes, parton a' from the resolved photon emitted by parton a of nucleus A interacts with the parton from nucleus B via the quark-antiquark annihilation and quark-gluon Compton scattering. The invariant cross section for large-p_T dilepton production by the inel.res-fra. is given by

$$\frac{d\sigma^{\text{inel.res.}}_{AB\to\ell^+\ell^-X}}{dM^2dp_T^2dy} = 2\int dx_a dx_b dz_a f_A(x_a,Q^2) f_B(x_b,Q^2) \times f_{\gamma/q}(z_a) f_\gamma(z'_a,Q^2)\frac{x_a x_b z_a z'_a}{x_a x_b z_a - x_a z_a x_2}\frac{\alpha}{3\pi M^2} \times\sqrt{1-\frac{4m_\ell^2}{M^2}}\left(1+\frac{2m_\ell^2}{M^2}\right)\frac{d\hat\sigma_{a'b\to\gamma^* d}}{d\hat t}, \quad (14)$$

where z'_a is the momentum fraction of the parton from the resolved photon.

B. Fragmentation dilepton production

We investigate the fragmentation processes which include the effect of the energy loss of hard partons traversing the hot-dense QGP for the large-p_T dilepton production. Jet quenching was a powerful tool to investigate properties of the dense medium. Energy loss of the parton before fragmenting into hadrons will modify the fragmentation function. It leads to a suppression of single-particle inclusive spectra. Considering in our calculation the fragmentation dileptons can be produced by the initial parton hard scattering, elastic two-photon processes (el.dou-fra.), semielastic processes, and inelastic photoproduction processes which include the effect of jet quenching.

The invariant cross section of fragmentation dileptons produced by the dir-fra. is given by

$$\frac{d\sigma^{\text{dir-fra.}}_{AB\to\ell^+\ell^-X}}{dM^2dp_T^2dy} = \int dx_a dx_b f_A(x_a,Q^2) f_B(x_b,Q^2) \times\frac{x_a x_b}{x_a x_b - \tau}\frac{\alpha}{3\pi M^2}\sqrt{1-\frac{4m_\ell^2}{M^2}}\left(1+\frac{2m_\ell^2}{M^2}\right) \times\frac{z_c^*}{z_c}\frac{D_{\gamma^*/q}(z_c^*,Q^{*2})}{z_c}\frac{d\hat\sigma_{ab\to cd}}{d\hat t}, \quad (15)$$

where $D_{\gamma^*/q}(z_c^*,Q^{*2})$ is the virtual photon fragmentation function [11], $z_c^* = z_c/(1-\Delta E/p_c)$, $p_c^* = p_c - \Delta E$, and $\Delta E = [C_R\alpha_s/N(E)](L^2\mu^2/\lambda_g)\ln(E/\mu)$ is the energy loss of the jet [64–66], where $N(E) = 4$, $\mu = 0.5$ GeV, C_R is the color Casimir of the jet, and λ_g is the average gluon mean-free path. The factor z_c^*/z_c appears because of the in-medium modification of the virtual photon fragmentation function [67]. $d\hat\sigma_{ab\to cd}/d\hat t$ is the cross section for the subprocesses [8],

$$\frac{d\hat\sigma}{d\hat t}(qq'\to qq') = \frac{\pi\alpha_s^2}{\hat s^2}\frac{4}{9}\frac{\hat s^2+\hat u^2}{\hat t^2}, \quad (16)$$

$$\frac{d\hat\sigma}{d\hat t}(qq\to qq) = \frac{\pi\alpha_s^2}{\hat s^2}\left[\frac{4}{9}\left(\frac{\hat s^2+\hat u^2}{\hat t^2}+\frac{\hat t^2+\hat u^2}{\hat s^2}\right) - \frac{8}{27}\frac{\hat s^2}{\hat t\hat u}\right], \quad (17)$$

$$\frac{d\hat\sigma}{d\hat t}(q\bar q\to q'\bar q') = \frac{\pi\alpha_s^2}{\hat s^2}\frac{4}{9}\frac{\hat t^2+\hat u^2}{\hat s^2}, \quad (18)$$

$$\frac{d\hat{\sigma}}{d\hat{t}}(q\bar{q} \to q\bar{q}) = \frac{\pi\alpha_s^2}{\hat{s}^2}\left[\frac{4}{9}\left(\frac{\hat{s}^2+\hat{u}^2}{\hat{t}^2}+\frac{\hat{t}^2+\hat{u}^2}{\hat{s}^2}\right)-\frac{8}{27}\frac{\hat{s}^2}{\hat{t}\hat{u}}\right], \tag{19}$$

$$\frac{d\hat{\sigma}}{d\hat{t}}(q\bar{q} \to gg) = \frac{\pi\alpha_s^2}{\hat{s}^2}\left[\frac{32}{27}\frac{\hat{s}^2+\hat{u}^2}{\hat{t}\hat{u}}-\frac{8}{3}\frac{\hat{t}^2+\hat{u}^2}{\hat{s}^2}\right], \tag{20}$$

$$\frac{d\hat{\sigma}}{d\hat{t}}(qg \to qg) = \frac{\pi\alpha_s^2}{\hat{s}^2}\left[-\frac{4}{9}\frac{\hat{s}^2+\hat{u}^2}{\hat{s}\hat{u}}+\frac{\hat{s}^2+\hat{u}^2}{\hat{t}^2}\right], \tag{21}$$

$$\frac{d\hat{\sigma}}{d\hat{t}}(gg \to q\bar{q}) = \frac{\pi\alpha_s^2}{\hat{s}^2}\left[\frac{1}{6}\frac{\hat{t}^2+\hat{u}^2}{\hat{t}\hat{u}}-\frac{3}{8}\frac{\hat{t}^2+\hat{u}^2}{\hat{s}^2}\right], \tag{22}$$

$$\frac{d\hat{\sigma}}{d\hat{t}}(gg \to gg) = \frac{\pi\alpha_s^2}{\hat{s}^2}\left[\frac{9}{2}\left(3-\frac{\hat{t}\hat{u}}{\hat{s}^2}-\frac{\hat{s}\hat{u}}{\hat{t}^2}-\frac{\hat{s}\hat{t}}{\hat{u}^2}\right)\right], \tag{23}$$

where α_s is the running coupling constant.

The invariant cross section of fragmentation dileptons produced by the semi.dir-fra. and the semi.res-fra. can be written as

$$\frac{d\sigma^{\text{semi.dir-fra.}}_{AB\to\ell^+\ell^-X}}{dM^2dp_T^2dy} = 2\int dx_a dx_b f_{\gamma/A}(x_a) f_B(x_b,Q^2)\frac{x_a x_b}{x_a x_b-\tau}\frac{\alpha}{3\pi M^2}\sqrt{1-\frac{4m_\ell^2}{M^2}}\left(1+\frac{2m_\ell^2}{M^2}\right)\frac{z_c^*}{z_c}\frac{D_{\gamma^*/q}(z_c^*,Q^{*2})}{z_c}\frac{d\hat{\sigma}_{\gamma b\to cd}}{d\hat{t}}, \tag{24}$$

$$\begin{aligned}\frac{d\sigma^{\text{semi.res-fra.}}_{AB\to\ell^+\ell^-X}}{dM^2dp_T^2dy} = {}& 2\int dx_a dx_b dz_a f_{\gamma/A}(x_a) f_\gamma(z_a,Q^2) f_B(x_b,Q^2)\frac{x_a x_b z_a}{x_a x_b z_a-\tau}\frac{\alpha}{3\pi M^2}\\ &\times\sqrt{1-\frac{4m_\ell^2}{M^2}}\left(1+\frac{2m_\ell^2}{M^2}\right)\frac{z_c^*}{z_c}\frac{D_{\gamma^*/q}(z_c^*,Q^{*2})}{z_c}\frac{d\hat{\sigma}_{a'b\to cd}}{d\hat{t}},\end{aligned} \tag{25}$$

respectively, where z_c is is the momentum fraction of the final-state dilepton. The cross section of subprocess $d\hat{\sigma}_{\gamma b\to cd}/d\hat{t}$ is given by

$$\frac{d\hat{\sigma}}{d\hat{t}}(q\gamma \to qg) = \frac{8}{9}\frac{\pi\alpha\alpha_s e_f^2}{s^2}\left[-\frac{\hat{u}}{\hat{s}}-\frac{\hat{s}}{\hat{u}}\right], \tag{26}$$

$$\frac{d\hat{\sigma}}{d\hat{t}}(g\gamma \to q\bar{q}) = \frac{1}{3}\frac{\pi\alpha\alpha_s e_f^2}{s^2}\left[\frac{\hat{t}}{\hat{u}}+\frac{\hat{u}}{\hat{t}}\right], \tag{27}$$

where $\hat{s}=(p_a+p_b)^2$, $\hat{t}=(p_c-p_a)^2$, and $\hat{u}=(p_c-p_b)^2$ are the Mandelstam variables for the subprocesses.

The fragmentation dileptons produced by the el.dou-fra. satisfy the following invariant cross section:

$$\frac{d\sigma^{\text{el.dou-fra.}}_{AB\to\ell^+\ell^-X}}{dM^2dp_T^2dy} = \int dx_a dx_b \frac{dL}{dW^2}\frac{x_a x_b}{x_a x_b-\tau}\frac{\alpha}{3\pi M^2}\sqrt{1-\frac{4m_\ell^2}{M^2}}\left(1+\frac{2m_\ell^2}{M^2}\right)\frac{D_{\gamma^*/q}(z_c,Q^2)}{z_c}\frac{d\hat{\sigma}_{\gamma\gamma\to cd}}{d\hat{t}}, \tag{28}$$

where dL/dW^2 is the two-photon luminosity given by [56,57]

$$\frac{dL}{dW^2} = \frac{16}{3}\frac{Z_1^2Z_2^2\alpha^2}{\pi^2W^2}\ln^3\left(\frac{2\gamma}{\sqrt{R_1R_2}W}\right), \tag{29}$$

with $W^2=4\omega_1\omega_2$ and $b_{1\,\min}=b_{2\,\min}=R_1+R_2$. The cross section for the subprocess is given by

$$\frac{d\hat{\sigma}}{d\hat{t}}(\gamma\gamma \to q\bar{q}) = \frac{2}{3}\frac{\pi\alpha^2 e_f^2}{\hat{s}^2}\left[\frac{\hat{t}}{\hat{u}}+\frac{\hat{u}}{\hat{t}}\right], \tag{30}$$

where $\hat{s}=(p_a+p_b)^2$, $\hat{t}=(p_c-p_a)^2$, and $\hat{u}=(p_c-p_b)^2$ are the Mandelstam variables for the subprocesses.

The invariant cross section of fragmentation dileptons produced by the inel.dir-fra., the inel.res-fra., and the inel.dou-fra. is given by

$$\begin{aligned}\frac{d\sigma^{\text{inel.dir-fra.}}_{AB\to\ell^+\ell^-X}}{dM^2dp_T^2dy} = {}& \int dx_a dx_b dz_a f_A(x_a,Q^2) f_B(x_b,Q^2) f_{\gamma/q}(z_a)\frac{x_a x_b z_a}{x_a x_b z_a-\tau}\frac{\alpha}{3\pi M^2}\sqrt{1-\frac{4m_\ell^2}{M^2}}\left(1+\frac{m_\ell^2}{M^2}\right)\\ &\times\frac{z_c^*}{z_c}\frac{D_{\gamma^*/q}(z_c^*,Q^{*2})}{z_c}\frac{d\hat{\sigma}_{\gamma b\to cd}}{d\hat{t}},\end{aligned} \tag{31}$$

$$\begin{aligned}\frac{d\sigma^{\text{inel.res-fra.}}_{AB\to\ell^+\ell^-X}}{dM^2dp_T^2dy} = {}& \int dx_a dx_b dz_a dz_a' f_A(x_a,Q^2) f_{\gamma/q}(z_a) f_\gamma(z_a',Q^2) f_B(x_b,Q^2)\frac{x_a x_b z_a z_a'}{x_a x_b z_a z_a'-\tau}\frac{\alpha}{3\pi M^2}\sqrt{1-\frac{4m_\ell^2}{M^2}}\\ &\times\left(1+\frac{m_\ell^2}{M^2}\right)\frac{z_c^*}{z_c}\frac{D_{\gamma^*/q}(z_c^*,Q^{*2})}{z_c}\frac{d\hat{\sigma}_{a'b\to cd}}{d\hat{t}},\end{aligned} \tag{32}$$

$$\frac{d\sigma^{\text{inel.dou-fra.}}_{AB\to\ell^+\ell^-X}}{dM^2dp_T^2dy} = \int dx_a dx_b dz_a dz_b f_A(x_a,Q^2) f_{\gamma/q}(z_a) f_B(x_b,Q^2) f_{\gamma/q}(z_b) \frac{x_a x_b z_a z_b}{x_a x_b z_a z_b - \tau} \frac{\alpha}{3\pi M^2}\sqrt{1-\frac{4m_\ell^2}{M^2}} \times \left(1+\frac{m_\ell^2}{M^2}\right)\frac{z_c^*}{z_c}\frac{D_{\gamma^*/q}(z_c^*,Q^{*2})}{z_c}\frac{d\hat{\sigma}_{\gamma\gamma\to cd}}{d\hat{t}}, \tag{33}$$

respectively, where $f_{\gamma/q}(x)$ is the equivalent photon spectrum function for the parton of the nucleus given by Eq. (13).

C. Large-p_T photon production

The prompt photons which do not come from the decay of large momentum hadrons can be divided into two categories: direct photons and fragmentation photons. The basic mechanisms of prompt photon production at the leading order are as follows: quark-antiquark annihilation ($q\bar{q}\to g\gamma$), quark-gluon Compton scattering ($qg\to q\gamma$), and bremsstrahlung radiation from the final-state parton ($q\to q\gamma$ and $g\to g\gamma$). In the elastic, semielastic, and inelastic photoproduction processes, the large-p_T real photons can be produced by the direct processes, resolved processes, and the fusion interaction of double photons and fragmentation processes.

Before the formation of hot-dense nuclear matter, the invariant cross section of the photons produced by hard collisions of high-energy initial partons is given by [9]

$$E\frac{d\sigma_{AB\to\gamma X}}{dp^3} = \frac{1}{\pi}\int dx_a f_A(x_a,Q^2) f_B(x_b,Q^2)\frac{x_a x_b}{x_a - x_1}\frac{d\hat{\sigma}_{ab\to\gamma d}}{d\hat{t}}, \tag{34}$$

where x_a and $x_b = x_a x_2/(x_a - x_1)$ are the parton's momentum fraction. The variables are $x_1 = \frac{1}{2}x_T\exp(y)$, $x_2 = \frac{1}{2}x_T\exp(-y)$, and $x_T = 2p_T/\sqrt{s}$. y is the rapidity. $d\hat{\sigma}/d\hat{t}(ab\to\gamma d)$ denotes the differential cross section of subprocesses [8],

$$\frac{d\hat{\sigma}}{d\hat{t}}(q\bar{q}\to\gamma g) = \frac{8}{9}\frac{\pi\alpha\alpha_s e_f^2}{\hat{s}^2}\left(\frac{\hat{t}}{\hat{u}}+\frac{\hat{u}}{\hat{t}}\right), \tag{35}$$

$$\frac{d\hat{\sigma}}{d\hat{t}}(q\bar{q}\to\gamma\gamma) = \frac{2}{3}\frac{\pi\alpha^2 e_f^4}{\hat{s}^2}\left(\frac{\hat{t}}{\hat{u}}+\frac{\hat{u}}{\hat{t}}\right), \tag{36}$$

$$\frac{d\hat{\sigma}}{d\hat{t}}(qg\to\gamma q) = \frac{1}{3}\frac{\pi\alpha\alpha_s e_f^2}{\hat{s}^2}\left(-\frac{\hat{u}}{\hat{s}}-\frac{\hat{s}}{\hat{u}}\right), \tag{37}$$

$$\begin{aligned}\frac{d\hat{\sigma}}{d\hat{t}}(gg\to\gamma\gamma) = \frac{\alpha^2\alpha_s^2}{8\pi\hat{s}^2}\left(\sum_{f=1}^{N_f}e_f^2\right)^2 \Bigg(\frac{1}{8}\Bigg\{&\left[\frac{\hat{s}^2+\hat{t}^2}{\hat{u}^2}\ln^2\left(\frac{-\hat{s}}{\hat{t}}\right)+2\frac{\hat{s}-\hat{t}}{\hat{u}}\ln\left(\frac{-\hat{s}}{\hat{t}}\right)\right]^2\\ &+\left[\frac{\hat{s}^2+\hat{u}^2}{\hat{t}^2}\ln^2\left(\frac{-\hat{s}}{\hat{u}}\right)+2\frac{\hat{s}-\hat{u}}{t}\ln\left(\frac{-\hat{s}}{\hat{u}}\right)\right]^2+\left[\frac{\hat{t}^2+\hat{u}^2}{\hat{s}^2}\ln^2\left(\frac{\hat{t}}{\hat{u}}\right)+2\frac{\hat{t}-\hat{u}}{\hat{s}}\ln\left(\frac{\hat{t}}{\hat{u}}\right)\right]^2\Bigg\}\\ &+\frac{1}{2}\Bigg[\frac{\hat{s}^2+\hat{t}^2}{\hat{u}^2}\ln^2\left(\frac{-\hat{s}}{\hat{t}}\right)+2\frac{\hat{s}-\hat{t}}{\hat{u}}\ln\left(\frac{-\hat{s}}{\hat{t}}\right)+\frac{\hat{s}^2+\hat{u}^2}{\hat{t}^2}\ln^2\left(\frac{-\hat{s}}{\hat{u}}\right)+2\frac{\hat{s}-\hat{u}}{\hat{t}}\ln\left(\frac{-\hat{s}}{\hat{u}}\right)\\ &+\frac{\hat{t}^2+\hat{u}^2}{\hat{s}^2}\ln^2\left(\frac{\hat{t}}{\hat{u}}\right)+2\frac{\hat{t}-\hat{u}}{\hat{s}}\ln\left(\frac{\hat{t}}{\hat{u}}\right)\Bigg]\\ &+\frac{\pi^2}{2}\left\{\left[\frac{\hat{s}^2+\hat{t}^2}{\hat{u}^2}\ln^2\left(\frac{-\hat{s}}{t}\right)+\frac{\hat{s}-\hat{t}}{\hat{u}}\right]^2+\left[\frac{\hat{s}^2+\hat{u}^2}{\hat{t}^2}\ln^2\left(\frac{-\hat{s}}{\hat{u}}\right)+\frac{\hat{s}-\hat{u}}{\hat{t}}\right]^2\right\}+4\Bigg),\end{aligned} \tag{38}$$

where α is the electromagnetic coupling constant, α_s is the running coupling constant, and N_f is the flavor of quarks.

The invariant cross section of large-p_T photons produced by the semi.dir-fra. and the semi.res-fra. can be written as

$$E\frac{d\sigma^{\text{semi.dir-fra.}}_{AB\to\gamma X}}{dp^3} = \frac{2}{\pi}\int dx_a f_{\gamma/N}(x_a) f_B(x_b,Q^2)\frac{x_a x_b}{x_a - x_1}\frac{d\hat{\sigma}_{\gamma b\to\gamma d}}{d\hat{t}}, \tag{39}$$

$$E\frac{d\sigma^{\text{semi.res-fra.}}_{AB\to\gamma X}}{dp^3} = \frac{2}{\pi}\int dx_a dx_b f_{\gamma/N}(x_a) f_B(x_b,Q^2) f_\gamma(z_a,Q^2)\frac{x_a x_b z_a}{x_a x_b - x_a x_2}\frac{d\hat{\sigma}_{a'b\to\gamma d}}{d\hat{t}}, \tag{40}$$

respectively, where z_a is the momentum fraction of the parton from the resolved photon and $d\hat{\sigma}/d\hat{t}(\gamma b \rightarrow \gamma d)$ denotes the differential cross section of subprocesses,

$$\frac{d\hat{\sigma}}{d\hat{t}}(q\gamma \rightarrow \gamma q) = \frac{2\pi\alpha^2 e_f^4}{\hat{s}^2}\left(-\frac{\hat{u}}{\hat{s}} - \frac{\hat{s}}{\hat{u}}\right), \tag{41}$$

where $\hat{s} = (p_a + p_b)^2$, $\hat{t} = (p_c - p_a)^2$, and $\hat{u} = (p_c - p_b)^2$ are the Mandelstam variables for the subprocesses.

The invariant cross section of large-p_T photons produced by the el.dou-fra. is given by

$$E\frac{d\sigma^{\text{el.dou-fra.}}_{AB\rightarrow\gamma X}}{dp^3} = \frac{1}{\pi}\int dx_a \frac{dL}{dW^2}\frac{x_a x_b}{x_a - x_1}\frac{d\hat{\sigma}_{\gamma\gamma\rightarrow\gamma d}}{d\hat{t}}, \tag{42}$$

where dL/dW^2 is the two-photon luminosity given in Eq. (29). The cross section for the subprocesses can be written as

$$\begin{aligned}\frac{d\hat{\sigma}}{d\hat{t}}(\gamma\gamma \rightarrow \gamma\gamma) = \frac{4\alpha^4}{\pi\hat{s}^2}\left(\sum_{f=1}^{N_f} e_f^2\right)^4 \Bigg(\frac{1}{8}\Bigg\{&\left[\frac{\hat{s}^2+\hat{t}^2}{\hat{u}^2}\ln^2\left(\frac{-\hat{s}}{\hat{t}}\right) + 2\frac{\hat{s}-\hat{t}}{\hat{u}}\ln\left(\frac{-\hat{s}}{\hat{t}}\right)\right]^2 \\ &+\left[\frac{\hat{s}^2+\hat{u}^2}{\hat{t}^2}\ln^2\left(\frac{-\hat{s}}{\hat{u}}\right) + 2\frac{\hat{s}-\hat{u}}{t}\ln\left(\frac{-\hat{s}}{\hat{u}}\right)\right]^2 + \left[\frac{\hat{t}^2+\hat{u}^2}{\hat{s}^2}\ln^2\left(\frac{\hat{t}}{\hat{u}}\right) + 2\frac{\hat{t}-\hat{u}}{\hat{s}}\ln\left(\frac{\hat{t}}{\hat{u}}\right)\right]^2\Bigg\} \\ &+\frac{1}{2}\Bigg[\frac{\hat{s}^2+\hat{t}^2}{\hat{u}^2}\ln^2\left(\frac{-\hat{s}}{\hat{t}}\right) + 2\frac{\hat{s}-\hat{t}}{\hat{u}}\ln\left(\frac{-\hat{s}}{\hat{t}}\right) + \frac{\hat{s}^2+\hat{u}^2}{\hat{t}^2}\ln^2\left(\frac{-\hat{s}}{\hat{u}}\right) + 2\frac{\hat{s}-\hat{u}}{\hat{t}}\ln\left(\frac{-\hat{s}}{\hat{u}}\right) + \frac{\hat{t}^2+\hat{u}^2}{\hat{s}^2}\ln^2\left(\frac{\hat{t}}{\hat{u}}\right) \\ &+2\frac{\hat{t}-\hat{u}}{\hat{s}}\ln\left(\frac{\hat{t}}{\hat{u}}\right)\Bigg] + \frac{\pi^2}{2}\left\{\left[\frac{\hat{s}^2+\hat{t}^2}{\hat{u}^2}\ln^2\left(\frac{-\hat{s}}{t}\right) + \frac{\hat{s}-\hat{t}}{\hat{u}}\right]^2 + \left[\frac{\hat{s}^2+\hat{u}^2}{\hat{t}^2}\ln^2\left(\frac{-\hat{s}}{\hat{u}}\right) + \frac{\hat{s}-\hat{u}}{\hat{t}}\right]^2\right\} + 4\Bigg),\end{aligned} \tag{43}$$

where α is the electromagnetic coupling constant, α_s is the running coupling constant, and N_f is the flavor of quarks.

The invariant cross section of large-p_T photons produced by the inel.dir-fra., the inel.res-fra., and the inelastic two-photon photoproduction (inel.dou.) can be written as

$$E\frac{d\sigma^{\text{inel.dir.}}_{AB\rightarrow\gamma X}}{dp^3} = \frac{2}{\pi}\int dx_a dx_b f_A(x_a,Q^2) f_B(x_b,Q^2) f_{\gamma/q}(z_a)\frac{x_a x_b z_a}{x_a x_b - x_a x_2}\frac{d\hat{\sigma}_{\gamma b\rightarrow\gamma d}}{d\hat{t}}, \tag{44}$$

$$E\frac{d\sigma^{\text{inel.res-fra.}}_{AB\rightarrow\gamma X}}{dp^3} = \frac{2}{\pi}\int dx_a dx_b dz_a f_A(x_a,Q^2) f_B(x_b,Q^2) f_{\gamma/q}(z_a) f_\gamma(z'_a,Q^2)\frac{x_a x_b z_a z'_a}{x_a x_b z_a - x_a z_a x_2}\frac{d\hat{\sigma}_{a'b\rightarrow\gamma d}}{d\hat{t}}, \tag{45}$$

$$E\frac{d\sigma^{\text{inel.dou.}}_{AB\rightarrow\gamma X}}{dp^3} = \frac{1}{\pi}\int dx_a dx_b dz_a f_A(x_a,Q^2) f_B(x_b,Q^2) f_{\gamma/q}(z_a) f_{\gamma/q}(z_b)\frac{x_a x_b z_a z_b}{x_a x_b z_a - x_a x_2}\frac{d\hat{\sigma}_{\gamma\gamma\rightarrow\gamma d}}{d\hat{t}}, \tag{46}$$

respectively, where z'_a is the momentum fraction of the parton from the resolved photon.

D. Fragmentation photon production

The invariant cross section for fragmentation photons produced by the dir-fra. is given by

$$E\frac{d\sigma^{\text{dir-fra.}}_{AB\rightarrow\gamma X}}{dp^3} = \frac{1}{\pi}\int dx_a dx_b f_A(x_a,Q^2) f_B(x_b,Q^2)\frac{z_c^*}{z_c}\frac{D_{\gamma/q}(z_c^*,Q^{*2})}{z_c}\frac{d\hat{\sigma}_{ab\rightarrow cd}}{d\hat{t}}, \tag{47}$$

where z_c is the momentum fraction of the final-state real photon, $D_{\gamma/q}(z_c^*,Q^{*2})$ is the real photon fragmentation function [8,10], $z_c^* = z_c/(1-\Delta E/p_c)$, $p_c^* = p_c - \Delta E$, and ΔE is the energy loss of the jet. The factor z_c^*/z_c appears because of the in-medium modification of the real photon fragmentation function [67].

The fragmentation photons produced by photoproduction processes can be divided into semielastic fragmentation processes and inelastic fragmentation processes.

The invariant cross section of fragmentation photons produced by the semi.dir-fra., the semi.res-fra., and the el.dou-fra. can be written as

$$E\frac{d\sigma^{\text{semi.dir-fra.}}_{AB\rightarrow\gamma X}}{dp^3} = \frac{2}{\pi}\int dx_a dx_b f_{\gamma/N}(x_a) f_B(x_b,Q^2)\frac{z_c^*}{z_c}\frac{D_{\gamma/q}(z_c^*,Q^{*2})}{z_c}\frac{d\hat{\sigma}_{\gamma b\rightarrow cd}}{d\hat{t}}, \tag{48}$$

$$E\frac{d\sigma^{\text{semi.res-fra.}}_{AB\rightarrow\gamma X}}{dp^3} = \frac{2}{\pi}\int dx_a dx_b dz_a f_{\gamma/N}(x_a) f_\gamma(z_a,Q^2) f_B(x_b,Q^2)\frac{z_c^*}{z_c}\frac{D_{\gamma/q}(z_c^*,Q^{*2})}{z_c}\frac{d\hat{\sigma}_{a'b\rightarrow cd}}{d\hat{t}}, \tag{49}$$

$$E\frac{d\sigma^{\text{el.dou-fra.}}_{AB\to\gamma X}}{dp^3}=\frac{1}{\pi}\int dx_a dx_b \frac{dL}{dW^2}\frac{D_{\gamma/q}(z_c^*,Q^{*2})}{z_c}\frac{z_c^*}{z_c}\frac{d\hat{\sigma}_{\gamma\gamma\to cd}}{d\hat{t}}, \tag{50}$$

respectively, where $dL/dW^2(x_a,x_b)$ is the two-photon luminosity given by Eq. (29).

The invariant cross section for fragmentation photons from the inel.dir-fra., the inel.res-fra., and the inel.dou-fra. can be written as

$$E\frac{d\sigma^{\text{inel.dir-fra.}}_{AB\to\gamma X}}{dp^3}=\frac{2}{\pi}\int dx_a dx_b dz_a f_A(x_a,Q^2) f_{\gamma/q}(z_a) f_B(x_b,Q^2)\frac{z_c^*}{z_c}\frac{D_{\gamma/q}(z_c^*,Q^{*2})}{z_c}\frac{d\hat{\sigma}_{\gamma b\to cd}}{d\hat{t}}, \tag{51}$$

$$E\frac{d\sigma^{\text{inel.res-fra.}}_{AB\to\gamma X}}{dp^3}=\frac{2}{\pi}\int dx_a dx_b dz_a dz_a' f_A(x_a,Q^2) f_{\gamma/q}(z_a) f_\gamma(z_a',Q^2) f_B(x_b,Q^2)\frac{z_c^*}{z_c}\frac{D_{\gamma/q}(z_c^*,Q^{*2})}{z_c}\frac{d\hat{\sigma}_{a'b\to cd}}{d\hat{t}}, \tag{52}$$

$$E\frac{d\sigma^{\text{inel.dou-fra.}}_{AB\to\gamma X}}{dp^3}=\frac{1}{\pi}\int dx_a dx_b dz_a dz_b f_A(x_a,Q^2)\frac{z_c^*}{z_c} f_{\gamma/q}(z_a) f_B(x_b,Q^2) f_{\gamma/q}(z_b)\frac{D_{\gamma/q}(z_c^*,Q^{*2})}{z_c}\frac{d\hat{\sigma}_{\gamma\gamma\to cd}}{d\hat{t}}, \tag{53}$$

respectively, where z_a' is the momentum fraction of the parton from the resolved photon.

E. Jet-dilepton (photon) conversion

The dileptons and photons are considered to be a useful probe for the investigation of the evolution of the QGP due to their very long mean-free path. The jet-dilepton (photon) conversion turns into an important dilepton (photon) production source in the QGP. Jets crossing the hot and dense plasma will lose their energy. Induced gluon bremsstrahlung, rather than elastic scattering of partons, is the dominant contribution of the jet energy loss [28,29,68,69]. Quark jets lose energy at less than half the rate as gluon jets, and the quark jets form the main fraction of jet events. The energy loss effect of jets before they convert into dileptons is found to be small, just about 20% [28]. Using the relativistic kinetic theory, we rigorously derive the production rate for the jet-dilepton (photon) conversion in the hot medium. We compare the contribution of the jet-medium interaction with the thermal emission and the Drell-Yan process.

In the central nucleus-nucleus collisions, the cross section of the Drell-Yan process for the dilepton production can be obtained as [19]

$$\frac{d\sigma^{DY}}{dM^2dy}=K\frac{4\pi\alpha^2}{9M^4}\sum_q e_q^2[x_a f_{q/A}(x_a,Q^2)x_b f_{\bar{q}/B}(x_b,Q^2)+x_a f_{\bar{q}/A}(x_a,Q^2)x_b f_{q/B}(x_b,Q^2)], \tag{54}$$

where $x_a=(M/\sqrt{s})\exp(y)$ and $x_b=(M/\sqrt{s})\exp(-y)$ are the momentum fractions. A K factor of 1.5 is used to account for the next-leading-order corrections.

The yield of thermal dileptons produced by quark-antiquark annihilation in the hot medium is given by [19,25,70]

$$\frac{dN^{\text{thermal}}}{dM^2d^4x}=\frac{\sigma(M)}{2(2\pi^4)}TM^3K_1\left(\frac{M}{T}\right), \tag{55}$$

where $K_1(x)=\sqrt{\pi/(2x)}\exp(-x)$ is the Bessel function.

The cross section of the $q\bar{q}\to\ell^+\ell^-$ interaction can be written as [19]

$$\sigma(M)=N_cN_s^2\sum_q e_q^2\frac{4\pi}{3}\frac{\alpha^2}{M^2}\sqrt{1-\frac{4m_\ell^2}{M^2}}\left(1+\frac{2m_\ell^2}{M^2}\right), \tag{56}$$

where $N_c=3$ and $N_s=2$ are the color and spin degeneracy of the quarks and m_ℓ is the mass of the lepton.

The fast quark jets passing through the hot and dense medium can produce large mass dileptons by annihilation with the thermal antiquarks. In the relativistic kinetic theory, the yield for the jet-dilepton conversion can be written as [34]

$$\frac{dN_{\text{jet}-\ell^+\ell^-}}{dM^2d^4x}=\frac{\sigma(M)M^2}{2(2\pi^4)}\int d|\mathbf{p}|f_{\text{jet}}(\mathbf{p})Te^{-M^2/4|\mathbf{p}|T}, \tag{57}$$

where $d^4x=\tau\,d\tau\,r\,dr\,d\eta\,d\phi$ is the space-time integration. In the Bjorken model, the initial temperature can be assigned by the transverse profile function as $T(r)=T_0[2(1-r^2/R_\perp^2)]^{1/4}$ with $R_\perp=1.2\ \text{Å}^{1/3}$ fm.

The phase-space distribution of the quark jets passing through the hot and dense quark-gluon plasma is given by [28,29,34]

$$f_{\text{jet}}(\mathbf{p})=\frac{1}{g_q}\frac{(2\pi)^3}{\pi R_\perp^2\tau p_\perp}\frac{dN_{\text{jet}}}{d^2p_\perp dy}R(r)\times\delta(\eta-y)\Theta(\tau_{\max}-\tau)\Theta(R_\perp-r), \tag{58}$$

where $g_q=6$ is the spin-color degeneracy of the parton, η is the space-time rapidity, $R(r)=2(1-r^2/R_\perp^2)$ is the transverse profile function, and $\tau_{\max}$ is smaller than the lifetime of the quark-gluon plasma and the time taken by the jet produced at position $\mathbf{r}$ to reach the surface of the quark-gluon plasma.

The jet spectrum for the nucleus-nucleus collisions is obtained by

$$\left.\frac{dN_{\text{jet}}}{d^2p_Tdy}\right|_{y=0}=T_{AA}\left.\frac{d\sigma_{\text{jet}}}{d^2p_Tdy}\right|_{y=0}, \tag{59}$$

where $T_{AA}=9\ \text{Å}^2/8\pi R_\perp^2$ is the nuclear thickness for the central collisions.

The invariant cross section for jets produced by the initial parton hard scattering processes (dir.) in hadronic collisions can be written as

$$\frac{d\sigma^{\text{dir.}}_{\text{jet}}}{d^2p_Tdy}=\frac{1}{\pi}\int dx_a f_A(x_a,Q^2)f_B(x_b,Q^2)\times\frac{x_ax_b}{x_a-x_1}\frac{d\hat{\sigma}_{ab\to cd}}{d\hat{t}}, \tag{60}$$

where x_a and $x_b = x_a x_2/(x_a - x_2)$ are the momentum fraction of the partons. The variables are $x_1 = \frac{1}{2}x_T \exp(y)$, $x_2 = \frac{1}{2}x_T \exp(-y)$, and $x_T = 2p_T\sqrt{s}$. $d\hat{\sigma}/d\hat{t}(ab \to cd)$ denotes the differential cross section of subprocesses.

At high energies, the fast jets can also be produced by the hard photoproduction processes. The invariant cross section of jets produced by the semi.dir-fra. and the semi.res. is given by

$$\frac{d\sigma_{\rm jet}^{\rm semi.dir.}}{d^2p_T dy} = \frac{2}{\pi}\int dx_a f_{\gamma/N}(x_a) f_B(x_b,Q^2) \times \frac{x_a x_b}{x_a - x_1}\frac{d\hat{\sigma}_{\gamma b\to cd}}{d\hat{t}}, \tag{61}$$

$$\frac{d\sigma_{\rm jet}^{\rm semi.res.}}{d^2p_T dy} = \frac{2}{\pi}\int dx_a dx_b f_{\gamma/N}(x_a) f_B(x_b,Q^2) \times f_\gamma(z_a,Q^2)\frac{x_a x_b z_a}{x_a x_b - x_a x_2}\frac{d\hat{\sigma}_{a'b\to cd}}{d\hat{t}}, \tag{62}$$

where z_a is the momentum fraction of the parton from the resolved photon.

The invariant cross section of jets produced by the inel.dir-fra., the inel.res-fra., and the inel.dou. can be written as

$$\frac{d\sigma_{\rm jet}^{\rm inel.dir.}}{d^2p_T dy} = \frac{2}{\pi}\int dx_a dx_b f_A(x_a,Q^2) f_B(x_b,Q^2) \times f_{\gamma/q}(z_a)\frac{x_a x_b z_a}{x_a x_b - x_a x_2}\frac{d\hat{\sigma}_{\gamma b\to cd}}{d\hat{t}}, \tag{63}$$

$$\frac{d\sigma_{\rm jet}^{\rm inel.res.}}{d^2p_T dy} = \frac{2}{\pi}\int dx_a dx_b dz_a f_A(x_a,Q^2) f_B(x_b,Q^2) \times f_{\gamma/q}(z_a) f_\gamma(z'_a,Q^2)\frac{x_a x_b z_a z'_a}{x_a x_b z_a - x_a z_a x_2}\frac{d\hat{\sigma}_{a'b\to cd}}{d\hat{t}}, \tag{64}$$

$$\frac{d\sigma_{\rm jet}^{\rm inel.dou.}}{d^2p_T dy} = \frac{1}{\pi}\int dx_a dx_b dz_a f_A(x_a,Q^2) f_B(x_b,Q^2) \times f_{\gamma/q}(z_a) f_{\gamma/q}(z_b)\frac{x_a x_b z_a z_b}{x_a x_b z_a - x_a x_2}\frac{d\hat{\sigma}_{\gamma\gamma\to cd}}{d\hat{t}}, \tag{65}$$

respectively, where z'_a is the momentum fraction of the parton from the resolved photon.

We investigate an important source of real photons originating from the passage of the high-energy jets through the quark-gluon plasma (jet-photon conversion). A fast jet passing through the quark-gluon plasma will interact with the thermal parton by quark-antiquark annihilation and quark-gluon Compton scattering. The yield of photon production by the quark-antiquark annihilation and quark-gluon Compton scattering in the hot-dense medium can be approximated as [17,19]

$$E\frac{dN^{(a)}}{d^3p\,d^4x} = \frac{\alpha\alpha_s N_s^2}{16\pi^2} f(\mathbf{p})T^2 \sum_q e_q^2\left[\ln\left(\frac{4ET}{m_{\rm th}^2}\right) + C\right], \tag{66}$$

$$E\frac{dN^{(C)}}{d^3p\,d^4x} = \frac{\alpha\alpha_s N_s N_\epsilon}{16\pi^2} f(\mathbf{p})T^2 \sum_q e_q^2\left[\ln\left(\frac{4ET}{m_{\rm th}^2}\right) + C'\right], \tag{67}$$

respectively, where $2m_{\rm th}^2 = g^2T^2/3$, $C = -1.916\,13$, $C' = -0.416\,13$, and $N_s = 2$ is the spin degeneracy of the quark, $N_\epsilon = 2$ is the spin degeneracy of the gluon, α is the electromagnetic coupling constant, and α_s is the strong running coupling constant. The phase-space distribution of the jets produced in a nuclear collision can be approximated as $f(\mathbf{p}) = f_{\rm th}(\mathbf{p}) + f_{\rm jet}(\mathbf{p})$, where $f_{\rm th}(\mathbf{p})$ is the thermal distribution of the partons in the hot-dense QGP [17,19] and $f_{\rm jet}(\mathbf{p})$ is the high-energy fast jets from the hard parton scattering processes and the photoproduction processes given in Eqs. (60)–(65).

III. LARGE-p_T LIGHT VECTOR MESON PRODUCTION

In relativistic heavy ion collisions, a complicated hadronic system with a large multiplicity of particles is formed, involving the possibility of QGP formation. The light vector meson appears to be a sensitive probe of quark-gluon plasma by using the pQCD calculation. Indeed, the strange quark component ($s\bar{s}$) of the ϕ meson makes its study interesting in connection with the strangeness enhancement observed in relativistic heavy ion collisions. In the present paper, we extend the photoproduction mechanism to the electromagnetic fragmentation production of the light vector meson in ultrarelativistic heavy ion collisions. The electromagnetic fragmentation function $D_{\gamma\to V}$ for a photon to split into a light vector meson V is given by [71,72]

$$D_{\gamma\to V} = \frac{3\Gamma_V^{e^+e^-}}{\alpha M_V}, \tag{68}$$

where α is the electromagnetic coupling constant and $\Gamma_V^{e^+e^-}$ and M_V are the electronic width and mass of the light vector meson, respectively.

A. Photoproduction processes in large-p_T light vector meson production

The light vector mesons can be produced by the initial parton collisions (the annihilation and Compton scattering of partons) and gluon-gluon fusion processes. The cross section for Drell-Yan-type inclusive light vector meson production in hadronic collisions can be written as

$$\frac{d\sigma_{AB\to VX}}{dp_T^2 dy} = \int dx_a f_A(x_a,Q^2) f_B(x_b,Q^2) \times \frac{x_a x_b}{x_a - x_1}\frac{d\hat{\sigma}_{ab\to\gamma d}}{d\hat{t}} D_{\gamma\to V}, \tag{69}$$

where x_a and $x_b = x_a x_2/(x_a - x_1)$ are the parton's momentum fraction. The variables are $x_1 = \frac{1}{2}x_T \exp(y)$, $x_2 = \frac{1}{2}x_T \exp(-y)$, and $x_T = 2p_T/\sqrt{s}$, and y is the rapidity. $d\hat{\sigma}/d\hat{t}(ab \to \gamma d)$ denotes the differential cross section of subprocesses.

The invariant cross section of large-p_T light vector mesons produced by the semi.dir-fra., the semi.res., and the el.dou-fra. can be written as

$$\frac{d\sigma_{AB\to VX}^{\rm semi.dir\text{-}fra.}}{dp_T^2 dy} = 2\int dx_a f_{\gamma/N}(x_a) f_B(x_b,Q^2) \times \frac{x_a x_b}{x_a - x_1}\frac{d\hat{\sigma}_{\gamma b\to\gamma d}}{d\hat{t}} D_{\gamma\to V}, \tag{70}$$

$$\frac{d\sigma^{\text{semi.res.}}_{AB\to VX}}{dp_T^2dy} = 2\int dx_a dx_b f_{\gamma/N}(x_a) f_B(x_b,Q^2) \times f_\gamma(z_a), Q^2 \frac{x_a x_b z_a}{x_a x_b - x_a x_2}\frac{d\hat{\sigma}_{a'b\to\gamma d}}{d\hat{t}} D_{\gamma\to V}, \tag{71}$$

$$\frac{d\sigma^{\text{el.dou-fra.}}_{AB\to VX}}{dp_T^2dy} = \int dx_a \frac{dL}{dW^2}\frac{x_a x_b}{x_a - x_1}\frac{d\hat{\sigma}_{\gamma\gamma\to\gamma d}}{d\hat{t}} D_{\gamma\to V}, \tag{72}$$

respectively, where z_a is the momentum fraction of the parton from the resolved photon.

The invariant cross section of large-p_T light vector mesons produced by the inel.dir-fra., the inel.res-fra., and the inel.dou. can be written as

$$\frac{d\sigma^{\text{inel.dir-fra.}}_{AB\to VX}}{dp_T^2dy} = 2\int dx_a dx_b f_A(x_a,Q^2) f_B(x_b,Q^2) \times f_{\gamma/q}(z_a)\frac{x_a x_b z_a}{x_a x_b - x_a x_2}\frac{d\hat{\sigma}_{\gamma b\to\gamma d}}{d\hat{t}} D_{\gamma\to V}, \tag{73}$$

$$\frac{d\sigma^{\text{inel.res-fra.}}_{AB\to VX}}{dp_T^2dy} = 2\int dx_a dx_b dz_a f_A(x_a,Q^2) f_B(x_b,Q^2) \times f_{\gamma/q}(z_a) f_\gamma(z'_a,Q^2)\frac{x_a x_b z_a z'_a}{x_a x_b z_a - x_a z_a x_2} \times \frac{d\hat{\sigma}_{a'b\to\gamma d}}{d\hat{t}} D_{\gamma\to V}, \tag{74}$$

$$\frac{d\sigma^{\text{inel.dou.}}_{AB\to VX}}{dp_T^2dy} = \int dx_a dx_b dz_a f_A(x_a,Q^2) f_B(x_b,Q^2) \times f_{\gamma/q}(z_a) f_{\gamma/q}(z_b)\frac{x_a x_b z_a z_b}{x_a x_b z_a - x_a x_2}\frac{d\hat{\sigma}_{\gamma\gamma\to\gamma d}}{d\hat{t}} D_{\gamma\to V}, \tag{75}$$

respectively, where z'_a is the momentum fraction of the parton from the resolved photon.

B. Fragmentation processes in large-p_T light vector meson production

The large-p_T direct photons can be used as the trigger for the light vector mesons. The trigger light vector mesons are produced by the fragmentation of partons that have also traversed the hot and dense medium and lose energy [36]. The invariant cross section for fragmentation photons produced by the dir-fra. is given by

$$\frac{d\sigma^{\text{dir-fra.}}_{AB\to VX}}{dp_T^2dy} = \int dx_a dx_b f_A(x_a,Q^2) f_B(x_b,Q^2) \times \frac{z_c^*}{z_c}\frac{D_{\gamma/q}(z_c^*,Q^{*2})}{z_c}\frac{d\hat{\sigma}_{ab\to cd}}{d\hat{t}} D_{\gamma\to V}, \tag{76}$$

where z_c is the momentum fraction of the final light vector meson, $D_{\gamma/q}(z_c^*,Q^{*2})$ is the real photon fragmentation function, $z_c^* = z_c/(1-\Delta E/p_c)$, $p_c^* = p_c - \Delta E$, and ΔE is the energy loss of the jet. The factor z_c^*/z_c appears because of the in-medium modification of the trigger photon fragmentation function [67]. The yield of light vector mesons depends on the production of the trigger photon [36].

The invariant cross section of fragmentation light vector mesons produced by the semi.dir-fra., the semi.res-fra., and the el.dou can be written as

$$\frac{d\sigma^{\text{semi.dir-fra.}}_{AB\to VX}}{dp_T^2dy} = 2\int dx_a dx_b f_{\gamma/N}(x_a) f_B(x_b,Q^2) \times \frac{z_c^*}{z_c}\frac{D_{\gamma/q}(z_c^*,Q^{*2})}{z_c}\frac{d\hat{\sigma}_{\gamma b\to cd}}{d\hat{t}} D_{\gamma\to V}, \tag{77}$$

$$\frac{d\sigma^{\text{semi.res-fra.}}_{AB\to VX}}{dp_T^2dy} = 2\int dx_a dx_b dz_a f_{\gamma/N}(x_a) f_\gamma(z_a,Q^2) \times f_B(x_b,Q^2)\frac{z_c^*}{z_c}\frac{D_{\gamma/q}(z_c^*,Q^{*2})}{z_c}\frac{d\hat{\sigma}_{a'b\to cd}}{d\hat{t}} D_{\gamma\to V}, \tag{78}$$

$$E\frac{d\sigma^{\text{el.dou-fra.}}_{AB\to VX}}{dp_T^2dy} = \int dx_a dx_b \frac{dL}{dW^2}\frac{D_{\gamma/q}(z_c^*,Q^{*2})}{z_c} \times \frac{z_c^*}{z_c}\frac{d\hat{\sigma}_{\gamma\gamma\to cd}}{d\hat{t}} D_{\gamma\to V}, \tag{79}$$

respectively, where $dL/dW^2(x_a,x_b)$ is the two-photon luminosity given by Eq. (29).

The invariant cross section for fragmentation light vector mesons based on the inel.dir-fra., the inel.res-fra., and the inel.dou-fra. can be written as

$$\frac{d\sigma^{\text{inel.dir-fra.}}_{AB\to VX}}{dp_T^2dy} = 2\int dx_a dx_b dz_a f_A(x_a,Q^2) f_B(x_b,Q^2) \times f_{\gamma/q}(z_a)\frac{z_c^*}{z_c}\frac{D_{\gamma/q}(z_c^*,Q^{*2})}{z_c}\frac{d\hat{\sigma}_{\gamma b\to cd}}{d\hat{t}} D_{\gamma\to V}, \tag{80}$$

$$\frac{d\sigma^{\text{inel.res-fra.}}_{AB\to VX}}{dp_T^2dy} = 2\int dx_a dx_b dz_a dz'_a f_A(x_a,Q^2) \times f_{\gamma/q}(z_a) f_\gamma(z'_a,Q^2) f_B(x_b,Q^2)\frac{z_c^*}{z_c} \times \frac{D_{\gamma/q}(z_c^*,Q^{*2})}{z_c}\frac{d\hat{\sigma}_{a'b\to cd}}{d\hat{t}} D_{\gamma\to V}, \tag{81}$$

$$\frac{d\sigma^{\text{inel.dou-fra.}}_{AB\to VX}}{dp_T^2dy} = \int dx_a dx_b dz_a dz_b f_A(x_a,Q^2) f_{\gamma/q}(z_a) \times f_B(x_b,Q^2) f_{\gamma/q}(z_b)\frac{z_c^*}{z_c}\frac{D_{\gamma/q}(z_c^*,Q^{*2})}{z_c} \times \frac{d\hat{\sigma}_{\gamma\gamma\to cd}}{d\hat{t}} D_{\gamma\to V}, \tag{82}$$

respectively, where z'_a is the momentum fraction of the parton from the resolved photon.

C. Jet-medium interaction processes in large-p_T light vector meson production

The associated light vector mesons are produced from the jet-medium interaction of the surviving jets after their passing through the hot and dense nuclear medium, whereas the trigger photons may come from the jet-photon conversion in relativistic heavy ion collisions. Hence, the light vector meson production in the hot and dense nuclear medium will depend on the jet-photon conversion at the production vertex as well as on the energy loss of the jets during their propagation in the nuclear medium [13,36,73]. The yield of light vector meson production by the quark-antiquark annihilation and quark-gluon Compton scattering in the hot-dense medium can be approximated as

$$E' \frac{dN_{\text{jet}-V}}{d^3p' d^4x} = \left(E \frac{dN^{(a)}}{d^3p\, d^4x} + E \frac{dN^{(C)}}{d^3p\, d^4x} \right) D_{\gamma\to V}, \tag{83}$$

where $D_{\gamma\to V}$ is the electromagnetic fragmentation function for a photon to split into a light vector meson given in Eq. (68). $E\, dN^{(a)}/d^3p\, d^4x$ and $E\, dN^{(C)}/d^3p\, d^4x$ are the yield of trigger photons given in Eqs. (66) and (67), respectively.

IV. NUMERICAL RESULTS

At high energies, the equivalent photon spectrum obtained from semiclassical description of high-energy electromagnetic collisions for the nucleus is $f_{\gamma/N} \propto Z^2 \ln \gamma$, the relativistic factor $\gamma = E/m_N = \sqrt{s}/2m_N \gg 1$ becomes very large at Large Hadron Collider energies. Indeed, the proton equivalent photon function obtained from Weizsäcker-Williams approximation is $f_{\gamma/p} \propto \ln A \propto \ln(s/m_p^2)$, where m_p is the proton mass. Since the collision energy $\sqrt{s}$ at the Large Hadron Collider is very large, the photon spectrum becomes important. Therefore the contribution of semielastic photoproduction processes is evident at Large Hadron Collider energies. For the inelastic photoproduction processes, the equivalent photon spectrum for the charged parton is $f_{\gamma/q} \propto \ln(E/m_q) = \ln(\sqrt{s}/2m_q) + \ln(x)$, where m_q is the charged parton mass. Hence the photon spectrum for the charged parton becomes prominent at Large Hadron Collider energies. The numerical results of our calculation for dileptons, photons, and light vector meson production produced by the hard photoproduction processes in relativistic heavy ion collisions are plotted in Figs. 1–12.

In Figs. 1–3, we plot the contribution of the dileptons produced by the semielastic and inelastic photoproduction processes for the mass range of 200 MeV $< M <$ 750 MeV in relativistic heavy ion collisions. In Figs. 1 and 2, the dilepton spectra of semielastic and inelastic photoproduction processes (the dotted line and dashed-dotted line) are compared with the dileptons spectra of the initial parton hard scattering processes (the dashed line) for p-p collisions and Pb-Pb collisions at the LHC, respectively. The contribution of the photoproduction processes is prominent at LHC energies. Indeed, the fragmentation dileptons produced by the semielastic and inelastic photoproduction processes (the dashed-dotted-dotted line and

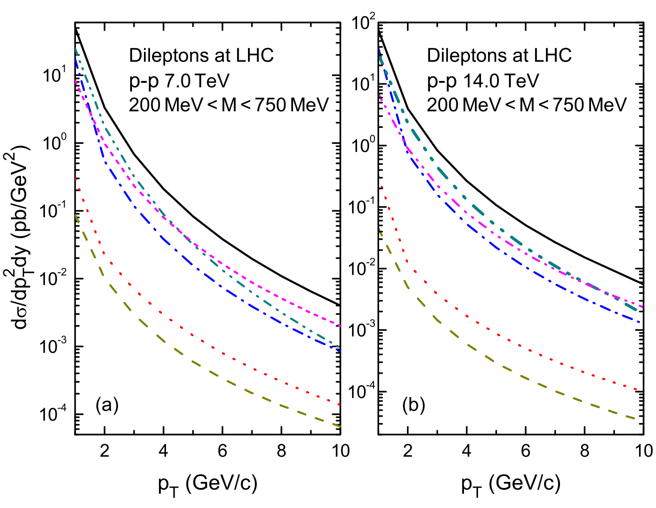

FIG. 1. (Color online) (a) The invariant cross section of large-p_T dilepton production for p-p collisions at $\sqrt{s} = 7.0$ TeV. The dashed line (dark yellow) is for the initial parton hard scattering processes [leading order (LO)], the dotted line (red) is for the semielastic photoproduction processes [semi.(dir.+res.)], the dashed-dotted line (blue) is for the inelastic photoproduction processes [inel.(dir.+res.+dou.)], the dashed-dotted-dotted line (dark cyan) is for the fragmentation dileptons produced by semielastic photoproduction processes [semi.(dir+res)-fra.], the short-dashed line (magenta) is for the fragmentation dileptons produced by inelastic photoproduction [inel.(dir+res+dou)-fra.], and the solid line (black) is for the sum of the above processes. (b) The same as panel (a) but for p-p collisions at $\sqrt{s} = 14.0$ TeV.

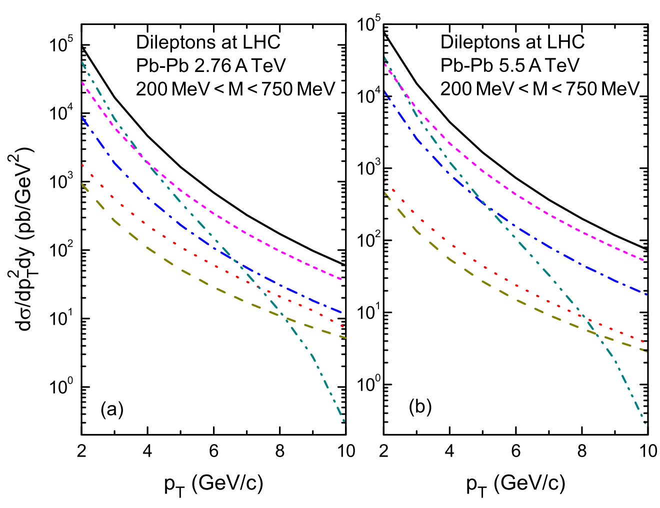

FIG. 2. (Color online) (a) The invariant cross section of large-p_T dilepton production for Pb-Pb collisions at $\sqrt{s} = 2.76$ TeV. The dashed line (dark yellow) is for the initial parton hard scattering processes (LO), the dotted line (red) is for the semielastic photoproduction processes [semi.(dir.+res.)], the dashed-dotted line (blue) is for the inelastic photoproduction processes [inel.(dir.+res.+dou.)], the dashed-dotted-dotted line (dark cyan) is for the fragmentation dileptons produced by semielastic photoproduction processes [semi.(dir+res)-fra.], the short-dashed line (magenta) is for the fragmentation dileptons produced by inelastic photoproduction [inel.(dir+res+dou)-fra.], and the solid line (black) is for the sum of the above processes. (b) The same as panel (a) but for Pb-Pb collisions at $\sqrt{s} = 5.5$ TeV.

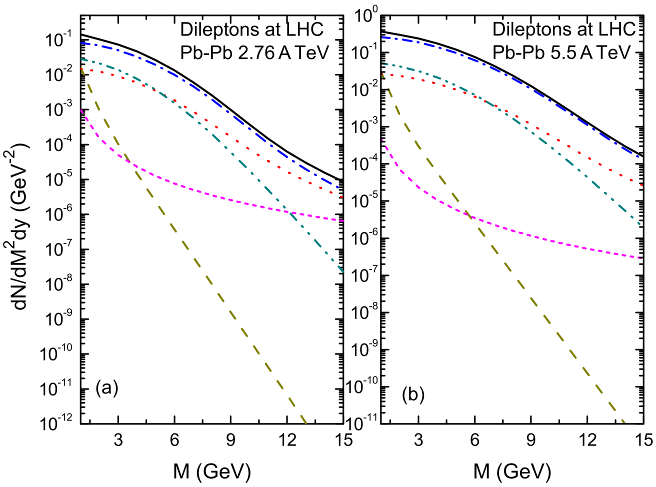

FIG. 3. (Color online) (a) The dilepton yield for Pb-Pb collisions with $\sqrt{s} = 2.76$ Å TeV. The dashed line (dark yellow) is for the thermal dilepton, the dotted line (red) is for the jet-dilepton conversion from the initial parton hard scattering processes, the dashed-doted line (blue) is for the jet-dilepton conversion from the inelastic photoproduction processes, the dashed-dotted-dotted line (dark cyan) is for the jet-dilepton conversion from the semielastic photoproduction processes, the short-dashed line (magenta) is for the Drell-Yan processes, and the solid line (black) is the sum of all the above processes. (b) The same as panel (a) but for Pb-Pb collisions at $\sqrt{s} = 5.5$ Å TeV.

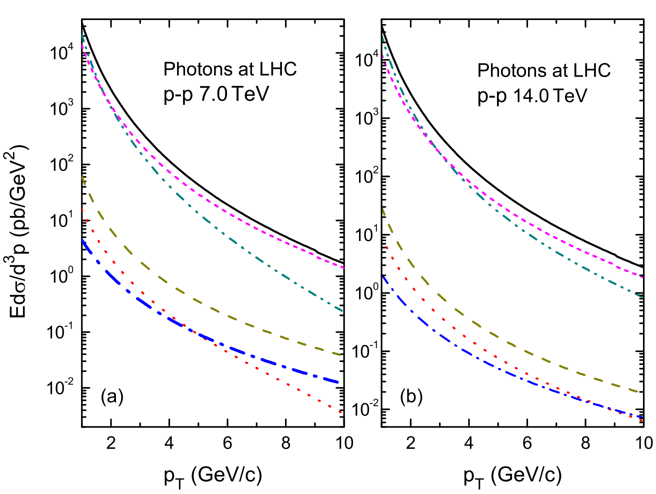

FIG. 4. (Color online) (a) The invariant cross section of large-p_T photon production for p-p collisions at $\sqrt{s} = 7.0$ TeV. The dashed line (dark yellow) is for the initial parton hard scattering processes (LO), the dotted line (red) is for the semielastic photoproduction processes [semi.(dir.+res.)], the dashed-dotted line (blue) is for the inelastic photoproduction processes [inel.(dir.+res.+dou.)], the dashed-dotted-dotted line (dark cyan) is for the fragmentation dileptons produced by semielastic photoproduction processes [semi.(dir+res)-fra.], the short-dashed line (magenta) is for the fragmentation dileptons produced by inelastic photoproduction [inel.(dir+res+dou)-fra.], and the solid line (black) is for the sum of the above processes. (b) The same as panel (a) but for p-p collisions at $\sqrt{s} = 14.0$ TeV.

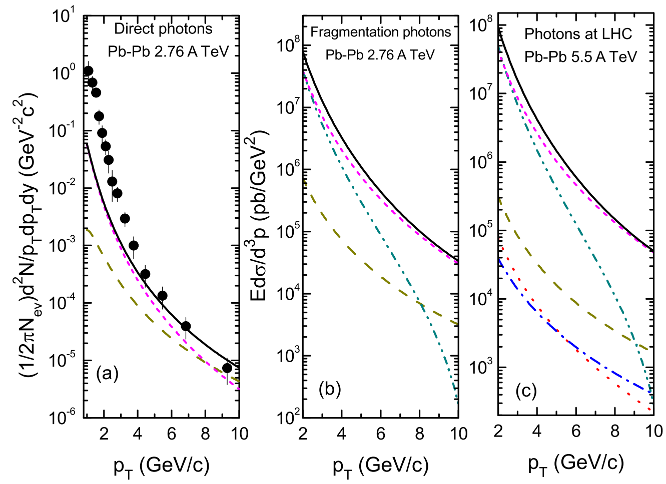

FIG. 5. (Color online) (a): The direct photon production in Pb-Pb collisions with $\sqrt{s} = 2.76$ Å TeV. The data points are from the ALICE Collaboration [2], the dashed line (dark yellow) is for the initial parton hard scattering processes (LO), the short-dashed line (magenta) is for the direct photons from photoproduction processes, and the solid line (black) is the sum all the above processes. (b) The fragmentation photon production in Pb-Pb collisions with $\sqrt{s} = 2.76$ Å TeV. The dashed line (dark yellow) is the initial parton hard scattering processes (LO), the dashed-dotted-dotted line (dark cyan) is for the semi-inelastic photoproduction processes, the short-dashed line (magenta) is for the inelastic photoproduction processes, and the solid line (black) is the sum. (c) The real photon production in Pb-Pb collisions with $\sqrt{s} = 5.5$ Å TeV. The dashed line (dark yellow) is for the initial parton hard scattering processes (LO), the dotted line (red) is for the semielastic photoproduction processes [semi.(dir.+res.)], the dashed-dot line (blue) is for the inelastic photoproduction processes [inel.(dir.+res.+dou.)], the dashed-dotted-dotted line (dark cyan) is for the fragmentation dileptons produced by semielastic photoproduction processes [semi.(dir+res)-fra.], the short-dashed line (magenta) is for the fragmentation dileptons produced by inelastic photoproduction [inel.(dir+res+dou)-fra.], and the solid line (black) is for the sum of the above processes.

short-dashed line) is evident in the region of $p_T > 2$ GeV for Pb-Pb collisions with $\sqrt{s} = 2.76$ and $\sqrt{s} = 5.5$ TeV. In Fig. 3, we plot the results for jet-dilepton conversion in the QGP. The fast jets produced by the semielastic and inelastic photoproduction processes passing through the thermal medium will lose their energies. Compared with the spectra of the Drell-Yan processes (the short-dashed line) and thermal dilepton (the dotted line), we find that the contribution of jet-dilepton conversion from semielastic and inelastic photoproduction processes (the dashed-dotted line and dashed-dotted-dotted line) is evident for $P_T > 4$ GeV in Pb-Pb collisions.

The spectra of real photons produced by the photoproduction processes are plotted in Figs. 4–6. Compared with the photons' spectra of the initial parton hard scattering processes (the dashed line), the contribution of photons produced by semielastic and inelastic photoproduction processes (the dotted line and dashed-dotted line) is prominent at LHC energies (Fig. 4). Furthermore, we compare with the ALICE Collaboration direct photon data [2] which has a big enhancement for $p_T < 4$ GeV in Fig. 5(a). We find that the

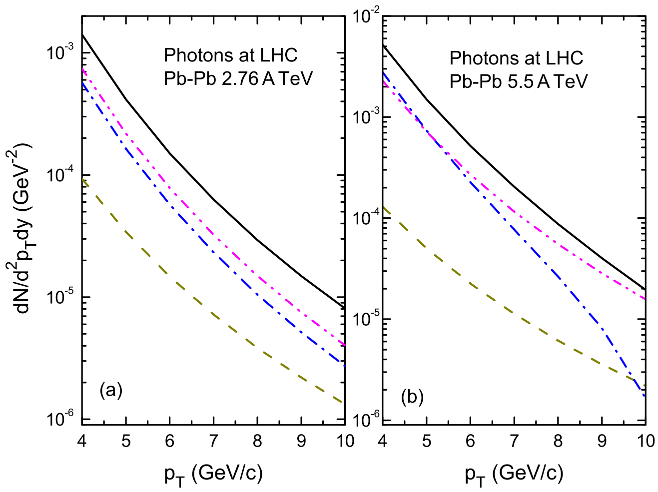

FIG. 6. (Color online) (a) The photon yield for Pb-Pb collisions with $\sqrt{s} = 2.76$ Å TeV. The dashed line (dark yellow) is for the jet-photon conversion from the initial parton hard scattering processes, the dashed-dotted line (blue) is for the jet-photon conversion from the semielastic photoproduction processes, the dashed-dotted-dotted line (magenta) is for the jet-photon conversion from the inelastic photoproduction processes, and the solid line (black) is the sum of all the above processes. (b) The same as panel (a) but for Pb-Pb collisions at $\sqrt{s} = 5.5$ Å TeV.

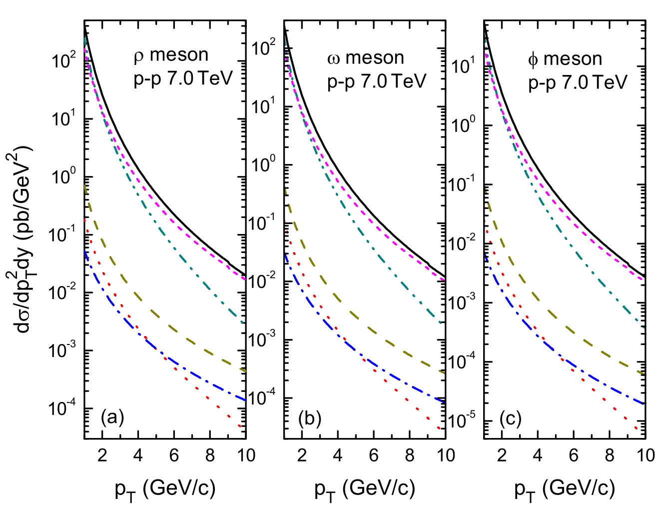

FIG. 7. (Color online) (a) The invariant cross section of ρ meson production for p-p collisions at $\sqrt{s} = 7.0$ TeV. The dashed line (dark yellow) is for the initial parton hard scattering processes (LO), the dotted line (red) is for the semielastic photoproduction processes [semi.(dir.+res.)], the dashed-dotted line (blue) is for the inelastic photoproduction processes [inel.(dir.+res.+dou.)], the dashed-dotted-dotted line (dark cyan) is for the ρ meson produced by semielastic photoproduction fragmentation processes [semi.(dir+res)-fra.], the short-dashed line (magenta) is for the ρ meson produced by inelastic photoproduction fragmentation processes [inel.(dir+res+dou)-fra.], and the solid line (black) is for the sum of the above processes. (b) The same as panel (a) but for ω meson production. (c) The same as panel (a) but for ϕ meson production.

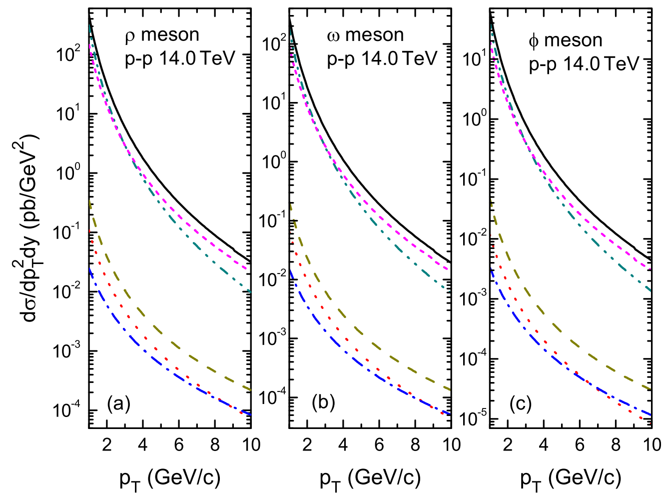

FIG. 8. (Color online) The same as Fig. 7 but for the light vector meson production in p-p collisions with $\sqrt{s} = 14.0$ TeV.

contribution of direct photons produced by photoproduction processes (the dashed-dotted line) cannot be negligible for Pb-Pb collisions with $\sqrt{s} = 2.76$ TeV [Fig. 5(a)]. Indeed, the contribution for fragmentation photons produced by the semielastic and inelastic photoproduction processes (the dashed-dotted-dotted line and short-dashed line) is evident in p-p and Pb-Pb collisions [Figs. 4, 5(b), and 5(c)]. For the thermal photons, the contribution from the semielastic and inelastic photoproduction processes (the dashed-dot line and

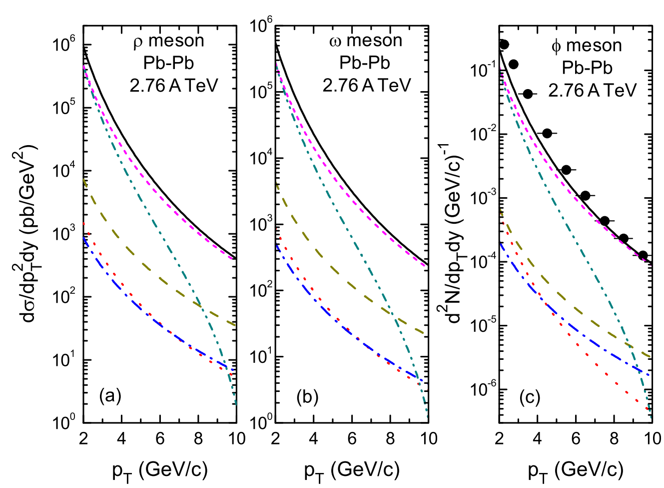

FIG. 9. (Color online) (a) The invariant cross section of ρ meson production for p-p collisions at $\sqrt{s} = 7.0$ TeV. The dashed line (dark yellow) is for the initial parton hard scattering processes (LO), the dotted line (red) is for the semielastic photoproduction processes [semi.(dir.+res.)], the dashed-dotted line (blue) is for the inelastic photoproduction processes [inel.(dir.+res.+dou.)], the dashed-dotted-dotted line (dark cyan) is for the ρ meson produced by semielastic photoproduction fragmentation processes [semi.(dir+res)-fra.], the short-dashed line (magenta) is for the ρ meson produced by inelastic photoproduction fragmentation processes [inel.(dir+res+dou)-fra.], and the solid line (black) is for the sum of the above processes. (b) The same as panel (a) but for ω meson production. (c) The same as panel (a) but for ϕ meson production. The ϕ meson data points are from the ALICE Collaboration [5].

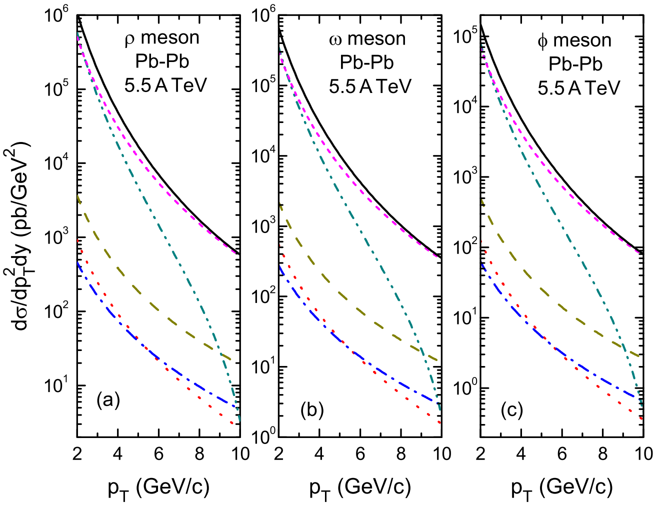

FIG. 10. (Color online) The same as Fig. 9 but for the light vector meson production in Pb-Pb collisions with $\sqrt{s} = 5.5$ Å TeV.

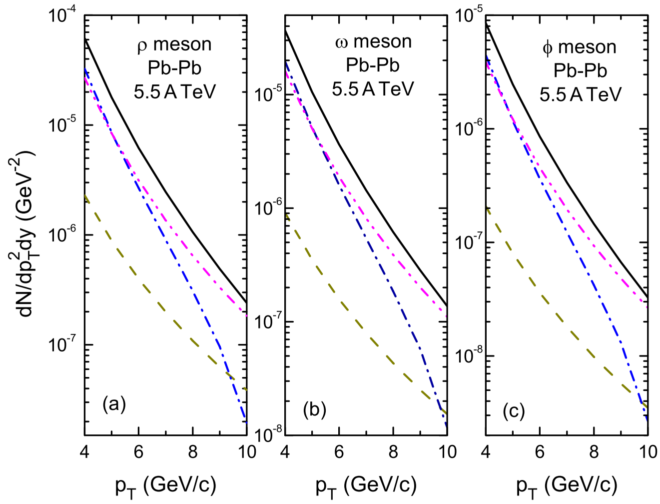

FIG. 12. (Color online) The same as Fig. 11 but for the light vector meson production in Pb-Pb collisions with $\sqrt{s} = 5.5$ Å TeV.

dashed-dotted-dotted line) becomes evident for $p_T > 4$ GeV in Pb-Pb collisions (Fig. 6).

We also plot the spectra of light vector mesons produced by the photoproduction processes in Figs. 7–12. Compared with the production cross section of the initial parton hard scattering processes (the dashed line), the contribution of light vector mesons produced by semielastic and inelastic photoproduction processes (the dotted line and dashed-dotted line) is prominent at LHC energies (Figs. 7–10). Indeed, the contribution for light vector mesons produced by the semielastic and inelastic photoproduction fragmentation processes (dashed-dotted-dotted line and short-dashed line) is evident in p-p and Pb-Pb collisions (Figs. 7–10). Furthermore, we compare with the ALICE Collaboration ϕ meson data [5] for Pb-Pb collisions in Fig. 9(c). We find that the contribution of a ϕ meson produced by photoproduction processes cannot be negligible for Pb-Pb collisions with $\sqrt{s} = 2.76$ TeV [Fig. 9(c)]. The contribution for light vector mesons produced by the jet-medium interaction based on the semielastic and inelastic photoproduction processes (the dashed-dotted line and dashed-dotted-dotted line) becomes evident for $p_T > 4$ GeV in Pb-Pb collisions (Figs. 11 and 12).

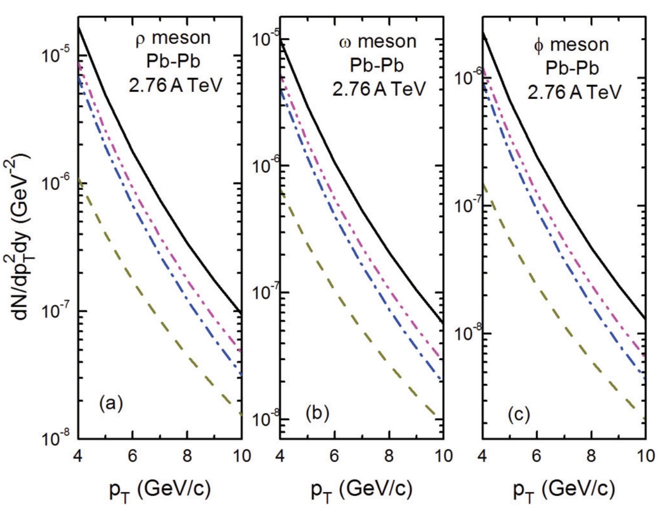

FIG. 11. (Color online) (a) The ρ meson yield for Pb-Pb collisions with $\sqrt{s} = 2.76$ Å TeV. The dashed line (dark yellow) is for the jet-medium interaction that the jet produced by the initial parton hard scattering processes, the dashed-dotted line (blue) is for the jet-medium interaction that the jet produced by the semielastic photoproduction processes, the dashed-dotted-dotted line (magenta) is for the the jet-medium interaction that the jet produced by the inelastic photoproduction processes, and the solid line (black) is the sum of all the above processes. (b) The same as panel (a) but for ω meson production. (c) The same as panel (a) but for ϕ meson production.

V. CONCLUSION

We have investigated the production of dileptons, real photons, and light vector mesons by the direct and resolved photoproduction processes in p-p collisions with $\sqrt{s} = 7$ and $\sqrt{s} = 14$ TeV and Pb-Pb collisions with $\sqrt{s} = 2.76$ and $\sqrt{s} = 5.5$ TeV. At the early stages of relativistic heavy ion collisions, the incident nucleus or the charged parton of the incident nucleus can emit large-p_T photons, then the high-energy photons interact with the partons of another incident nucleon by the quantum electrodynamics Compton scattering and photon-gluon fusion. Furthermore, the hadronlike photons also can interact with the partons of the nucleus by annihilation and Compton scattering. Indeed, the fast jets produced by the direct and resolved photoproduction processes pass through the hot and dense plasma and interact with the thermal partons of the quark-gluon plasma. The numerical results for photoproduction processes can improve the contribution of dileptons, photons, and light vector mesons production in p-p and Pb-Pb collisions at LHC energies.

ACKNOWLEDGMENTS

This work was supported by the National Natural Science Foundation of China under Grants No. 11465021 and No. 11065010.

[1] ALICE Collaboration, R. Ichou *et al.*, Nucl. Phys. A **855**, 339 (2011).
[2] ALICE Collaboration, M. Wilde *et al.*, Nucl. Phys. A **904-905**, 573c (2013).
[3] ALICE Collaboration, M. K. Koehler *et al.*, arXiv:1302.2049 [hep-ex].
[4] ALICE Collaboration, B. Abelev *et al.*, Eur. Phys. J. C **72**, 2183 (2012).
[5] ALICE Collaboration, A. G. Knospe *et al.*, EPJ Web Conf. **36**, 00013 (2012).
[6] CMS Collaboration, V. Khachatryan *et al.*, Phys. Rev. Lett. **106**, 082001 (2011).
[7] CMS Collaboration, S. Chatrchyan *et al.*, J. High Energy Phys. 11 (2012) 080.
[8] J. F. Owens, Rev. Mod. Phys. **59**, 465 (1987).
[9] R. D. Field, *Applications of Perturbative QCD* (Addison-Wesley, Reading, MA, 1989).
[10] S. Turbide, C. Gale, S. Jeon, and G. D. Moore, Phys. Rev. C **72**, 014906 (2005).
[11] Z.-B. Kang, J.-W. Qiu, and W. Vogelsang, Phys. Rev. D **79**, 054007 (2009).
[12] Z.-B. Kang, J.-W. Qiu, and W. Vogelsang, Nucl. Phys. A **830**, 571c (2009).
[13] X.-N. Wang, Phys. Lett. B **595**, 165 (2004).
[14] M. Glück, E. Reya, and A. Vogt, Phys. Rev. D **46**, 1973 (1992).
[15] D. d'Enterria and G. G. da Silveira, Phys. Rev. Lett. **111**, 080405 (2013).
[16] Z. Bern, A. De Freitas, A. Ghinculov, H. Wong, and L. Dixon, J. High Energy Phys. 11 (2001) 031.
[17] J. Kapusta, P. Lichard, and D. Seibert, Phys. Rev. D **44**, 2774 (1991).
[18] J. D. Bjorken, Phys. Rev. D **27**, 140 (1983).
[19] C.-Y. Wong, *Introduction to High Energy Heavy-Ion Collisions* (World Scientific, Singapore, 1994).
[20] E. Shuryak and L. Xiong, Phys. Rev. Lett. **70**, 2241 (1993).
[21] E. V. Shuryak and I. Zahed, Phys. Rev. C **70**, 021901(R) (2004).
[22] M. Dion, J.-F. Paquet, B. Schenke, C. Young, S. Jeon, and C. Gale, Phys. Rev. C **84**, 064901 (2011).
[23] H. van Hees, C. Gale, and R. Rapp, Phys. Rev. C **84**, 054906 (2011).
[24] S. Turbide, R. Rapp, and C. Gale, Phys. Rev. C **69**, 014903 (2004).
[25] J. K. Nayak, J. Alam, S. Sarkar, and B. Sinha, Phys. Rev. C **78**, 034903 (2008).
[26] C. M. Hung and E. V. Shuryak, Phys. Rev. C **56**, 453 (1997).
[27] L. G. Landsberg, Phys. Rep. **128**, 301 (1985).
[28] R. J. Fries, B. Müller, and D. K. Srivastava, Phys. Rev. Lett. **90**, 132301 (2003).
[29] R. J. Fries, B. Müller, and D. K. Srivastava, Phys. Rev. C **72**, 041902(R) (2005).
[30] S. Turbide, C. Gale, E. Frodermann, and U. Heinz, Phys. Rev. C **77**, 024909 (2008).
[31] D. K. Srivastava, C. Gale, and R. J. Fries, Phys. Rev. C **67**, 034903 (2003).
[32] F.-M. Liu, T. Hirano, K. Werner, and Y. Zhu, Phys. Rev. C **79**, 014905 (2009).
[33] Y.-P. Fu and Y.-D. Li, Phys. Rev. C **84**, 044906 (2011).
[34] Y.-P. Fu and Y.-D. Li, Nucl. Phys. A **865**, 76 (2011).
[35] G.-Y. Qin, C. Gale, S. Jeon, G. D. Moore, and J. Ruppert, Nucl. Phys. A **830**, 459c (2009).
[36] G.-Y. Qin, J. Ruppert, C. Gale, S. Jeon, and G. D. Moore, Phys. Rev. C **80**, 054909 (2009).
[37] F. Gelis and J. Jalilian-Marian, Phys. Rev. D **66**, 094014 (2002).
[38] J. Jalilian-Marian and A. H. Rezaeian, Phys. Rev. D **86**, 034016 (2012).
[39] M. A. Betemps and M. B. Gay Ducati, Phys. Rev. D **70**, 116005 (2004).
[40] M. Chiu, T. K. Hemmick, V. Khachatryan, A. Leonidov, J. Liao, and L. McLerran, Nucl. Phys. A **900**, 16 (2013).
[41] L. McLerran and B. Schenke, Nucl. Phys. A **929**, 71 (2014).
[42] D. Y. Ivanov, M. I. Kotsky, and A. Papa, Eur. Phys. J. C **38**, 195 (2004).
[43] J. R. Forshaw, R. Sandapen, and G. Shaw, Phys. Rev. D **69**, 094013 (2004).
[44] R. Enberga, Nucl. Phys. A **755**, 595c (2005).
[45] B. Pire, L. Szymanowski, and S. Wallon, Eur. Phys. J. C **44**, 545 (2005).
[46] R. Engel and J. Ranft, Phys. Rev. D **54**, 4244 (1996).
[47] R. C. Hwa and C. B. Yang, Phys. Rev. C **75**, 054904 (2007).
[48] L.-W. Chen and C. M. Ko, Phys. Rev. C **73**, 044903 (2006).
[49] Y.-D. Li and L.-S. Liu, Phys. Lett. B **377**, 177 (1996).
[50] R. Nisius, Phys. Rep. **332**, 165 (2000).
[51] M. Krawczyk, A. Zembrzuski, and M. Staszel, Phys. Rep. **345**, 265 (2001).
[52] G.-M. Yu and Y.-D. Li, Chin. Phys. Lett. **30**, 011201 (2013).
[53] M. Glück, E. Reya, and A. Vogt, Z. Phys. C **53**, 127 (1992).
[54] X.-N. Wang and M. Gyulassy, Phys. Rev. D **44**, 3501 (1991).
[55] M. Glück, E. Reya, and I. Schienbein, Phys. Rev. D **60**, 054019 (1999).
[56] J. D. Jackson, *Classical Electrodynamics* (Wiley, New York, 1963).
[57] E. Papageorgiu, Phys. Lett. B **250**, 155 (1990).
[58] N. Baron and G. Baur, Phys. Rev. C **49**, 1127 (1994).
[59] M. Drees, R. M. Godbole, M. Nowakowski, and S. D. Rindani, Phys. Rev. D **50**, 2335 (1994).
[60] M. Drees and D. Zeppenfeld, Phys. Rev. D **39**, 2536 (1989).
[61] B. A. Kniehl, Phys. Lett. B **254**, 267 (1991).
[62] S. J. Brodsky, T. Kinoshita, and H. Terazawa, Phys. Rev. D **4**, 1532 (1971).
[63] H. Terazawa, Rev. Mod. Phys. **45**, 615 (1973).
[64] P. Lévai, G. Papp, G. Fai, M. Gyulassy, G. G. Barnaföldi, I. Vitev, and Y. Zhang, Nucl. Phys. A **698**, 631 (2002).
[65] M. Gyulassy, P. Lévai, and I. Vitev, Phys. Rev. Lett. **85**, 5535 (2000).
[66] M. Gyulassy, P. Lévai, and I. Vitev, Nucl. Phys. B **594**, 371 (2001).
[67] X.-N. Wang and Z. Huang, Phys. Rev. C **55**, 3047 (1997).
[68] M. Gyulassy and M. Plümer, Phys. Lett. B **243**, 432 (1990).
[69] X.-N. Wang, M. Gyulassy, and M. Plümer, Phys. Rev. D **51**, 3436 (1995).
[70] K. Kajantie, J. Kapusta, L. McLerran, and A. Mekjian, Phys. Rev. D **34**, 2746 (1986).
[71] M. Davier and M. Peskin, and A. Snyder, arXiv:hep-ph/0606155.
[72] S. Fleming, Phys. Rev. D **50**, 5808 (1994).
[73] X.-N. Wang, Phys. Lett. B **579**, 299 (2004).